Model-Based Residual Bootstrap of Constrained Spherical Deconvolution for Probabilistic Segmentation and Tractography

H. A. Haroon[1], D. M. Morris[1], K. V. Embleton[1,2], and G. J. Parker[1]

[1]Imaging Science and Biomedical Engineering, School of Cancer and Imaging Sciences, The University of Manchester, Manchester, England, United Kingdom,
[2]School of Psychological Sciences, The University of Manchester, Manchester, England, United Kingdom

Introduction We have recently presented the application of model-based residual bootstrapping (MRB) to the *q*-ball[1] analysis of DWI datasets[2]. Model-based residual bootstrap enables quantification of the uncertainty in the inferred fiber orientation for probabilistic fiber tracking using a single HARDI dataset[3,4,5]. Recently it has been shown that the constrained spherical deconvolution[6,7] (CSD) technique is able to estimate multiple intravoxel fiber orientations more accurately than *q*-ball[6,7]. Here we describe the application of MRB to the analysis of HARDI data using CSD. We present maps of observing *n* fiber orientations estimated by CSD MBR bootstrapping over 32 iterations on a voxel-by-voxel basis and show some examples of probabilistic tractography using orientation PDFs derived from the bootstrapping process.

Methods *Imaging:* HARDI data were acquired in a healthy subject on a 3T Philips Achieva scanner (Philips Medical Systems, Best, Netherlands) using an 8-element head coil. PGSE EPI with TE = 59 ms, cardiac gating, G_{max} = 62 mT/m, partial Fourier factor 0.679, 112 × 112 matrix reconstructed to 128 × 128, reconstructed resolution 1.875 × 1.875 mm^2, slice thickness 2.1 mm, 60 contiguous slices, 61 diffusion sensitisation directions at b = 1200s/mm^2 (Δ = 29.8ms, δ = 13.1ms), 1 at b = 0, SENSE factor = 2.5, correction for susceptibility and eddy current-induced distortion[8].

The imaging data was analysed with software developed and implemented in MATLAB (http://www.mathworks.com/products/matlab/).

Constrained Spherical Deconvolution: We implemented CSD[6,7] on the acquired HARDI data. The response function was obtained from the simulation of a single diffusion tensor with fractional anisotropy of 0.8 and b = 1200s/mm^2. The fiber orientation distribution (FOD) function was generated with 45 spherical harmonics (l_{max}=8) and was then reconstructed at 8000 equidistant points on the sphere, within each voxel. The signal-to-noise level of our data was too low to carry out super-resolution CSD[7].

MBR Bootstrapping: In order to obtain residuals in a given voxel we spherically convolved the spherical harmonics of the FOD generated by CSD with the rotational harmonics of the response function. This gave us recovered HARDI signal, devoid of noise. Residuals were calculated by taking the difference between the recovered HARDI signal and the original HARDI signal. A new image set was created by randomly shuffling the residuals, for any given voxel, amongst all the diffusion-encoding directions and then adding them on to the recovered HARDI signals. The image set created by each bootstrap sampling was then processed with CSD to generate new instances of the FODs. To further minimise the effects of noise we set a threshold to only accept those peaks on the FOD, as relating to the principle underlying intravoxel fiber orientations (one or more), whose magnitude was greater than 70% of the maximum peak magnitude on the FOD, in a given voxel. We used 32 bootstrap iterations and fit a local 2D quadratic function to the peaks on the FOD to give an interpolated estimate of the dominant underlying fiber orientations.

Probability Maps of Fiber Orientation: The probability of observing *n* fiber orientations was determined from the frequency of finding *n* fiber orientations over 32 MBR bootstrap iterations. We chose n = 1, 2, 3 and greater than 3.

Probabilistic Tractography: The fiber orientations estimated over 32 MBR bootstrap iterations in every voxel of the brain form a probability density function (PDF) for probabilistic tractography using PICo[9,10,11], with 1000 Monte Carlo streamlines. We used a single principle direction with high uncertainty in a voxel if the number of fiber orientations was greater than 3, on any bootstrap iteration. Example probabilistic fiber tracking was seeded from regions in the splenium of the corpus callosum (SCC) and the internal capsule (IC).

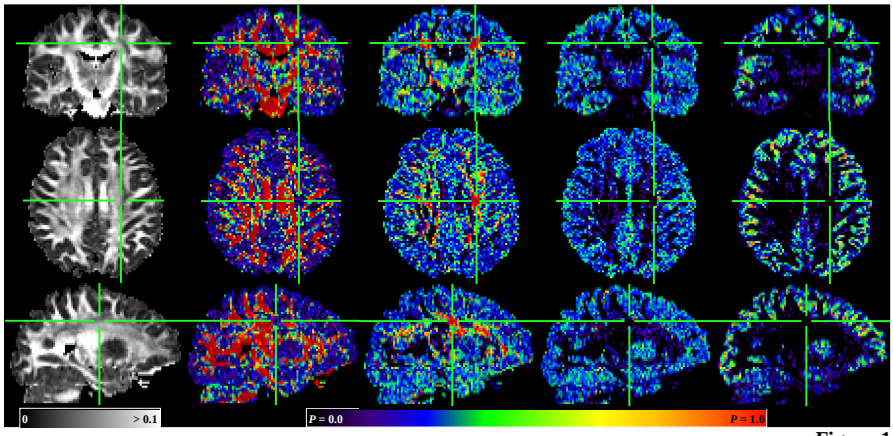

Figure 1

Results Figure 1 shows orthogonal views of the volume maps for the generalised fractional anisotropy (GFA) from *q*-ball[1] (Fig. 1 1st column), $P(n = 1)$ (Fig. 1 2nd column), $P(n = 2)$ (Fig. 1 3rd column), $P(n = 3)$ (Fig. 1 4th column) and $P(n > 3)$ (Fig. 1 5th column) over 32 MBR bootstrap iterations. The green crosshairs in Fig. 1 are centred on an area of white matter (Fig. 1 1st column) known to contain crossing fibers, which is identified as having a very high probability for n = 2 (Fig. 1 3rd column) but negligible probability on all the other maps. The rows of Figure 2 show the results of probabilistic tractography from the SCC (Fig. 2 A) and the IC (Fig. 2 B), overlaid on orthogonal 3D rendered views of the b = 0 volume. The light green areas are the regions used to seed the tracking from. Tracking demonstrates regions of high confidence, such as the internal capsule, and regions of greater tracking dispersion, as expected in regions of lower orientational confidence and fiber crossings.

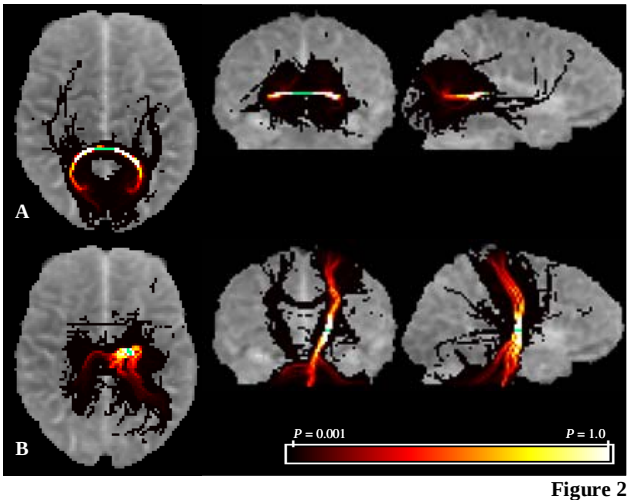

Figure 2

Conclusion We have successfully applied model-based residual bootstrapping to the CSD analysis of clinically-acquirable HARDI data. We demonstrate that the method is able to provide estimates of the probability of finding different fiber configurations within the brain. These distributions may then be used directly as PDFs across each configuration for probabilistic tractography. This method provides a means by which the microstructural complexity of tissue, as reflected in the HARDI diffusion signal, may be characterised, naturally accounting for the underlying tissue microscopic complexity, macroscopic partial volume, and data noise levels.

References 1. Tuch, DS, *Magn Reson Med*, **52**: 1358, 2004. 2. Haroon, HA, *et al*, *IEEE Trans Med Imaging*, in press, 2008. 3. Whitcher, B, *et al*, *Hum Brain Mapp*, 29: 346, 2008. 4. Jones, DK, *IEEE Trans Med Imaging*, **27**: 1268, 2008. 5. Berman, JI, *et al*, *NeuroImage*, **39**: 215, 2008. 6. Tournier, J-D, *et al*, *NeuroImage*, **35**: 1459, 2007. 7. Tournier, J-D, *et al*, *NeuroImage*, **42**: 617, 2008. 8. Embleton, KV, *et al*, *Proc ISMRM*, 1070, 2006. 9. Parker, GJ, & Alexander, DC, *Lect Notes Comput Sci*, **2732**: 684, 2003. 10. Parker, GJ, & Alexander, DC, *Phil Trans R Soc Series B*, **360**: 893, 2005. 11. Alexander, *et al*, *Magn Reson Med*, **48**:331, 2002.

Acknowledgements We would like to thank Dr Jacques-Donald Tournier (Brain Research Institute, Melbourne, Australia) for providing us with his original CSD code. The figures have been produced using MRIcro (http://www.sph.sc.edu/comd/rorden/mricro.html). This work is supported by the UK's BBSRC (BB/E002226/1), EPSRC (GR/T02669/01) and MRC (G0501632).